atmosphere

MDPI

Communication

The Dependence of Gales on Relevant Meteorological Elements in One of the Hottest Regions of China, the Turpan Basin

Zhiqi Xu [1,2], Hao Tang [2,*], Xiya Zhang [1] and Haibo Hu [1]

[1] Institute of Urban Meteorology, China Metrological Administration, Beijing 100089, China; xzqnuist@163.com (Z.X.); kuailenalu@163.com (X.Z.); hhbzy2001@sohu.com (H.H.)
[2] Xinjiang Meteorological Observatory, Urumqi 830002, China
* Correspondence: tanghao72@163.com

Abstract: The Turpan Basin is one of the hottest regions in China, with high fire potential. The occurrence of gales could roll over trains as well as spread and expand the fire rapidly, posing adverse effects on traffic and fire protection. Therefore, it is important to discuss the frequency and mechanism of gales in Turpan. Based on the observational data of seven stations and ERA5 reanalysis data from 2015 to 2021, this study uses the t-mode principal component analysis using the oblique rotation (T-PCA) method to explore the seasonal differences and related synoptic patterns of gales in the Turpan Basin. The synoptic circulations are divided into nine categories. In types 1, 2, 3, 5, 7 and 9, there are a high-pressure center to the west and a lower-pressure center to the south of Turpan, while in types 4, 6 and 8, there is a strong high-pressure center to the south or northeast of Turpan. When the high-pressure system is located to the west of Turpan, gales are prone to occur, while to the south or northeast, gales seem to be less likely to occur, which is closely related to synoptic patterns and terrain. To the best of our knowledge, this study pioneered the frequency and mechanism of gales in Turpan, which could facilitate gale prevention in the area.

Keywords: Turpan Basin; gales; T-PCA; high temperature

Citation: Xu, Z.; Tang, H.; Zhang, X.; Hu, H. The Dependence of Gales on Relevant Meteorological Elements in One of the Hottest Regions of China, the Turpan Basin. *Atmosphere* **2023**, *14*, 1051. https://doi.org/10.3390/atmos14061051

Academic Editor: Ferdinando Salata

Received: 12 April 2023
Revised: 12 June 2023
Accepted: 13 June 2023
Published: 19 June 2023

1. Introduction

Natural disasters constrain the sustainable development of a region. In recent years, natural disasters have occurred frequently around the world, and the disaster situation has continued to worsen, seriously affecting human life [1–4]. Winds with instantaneous speeds reaching or exceeding 10.8 m per second are called gales, and a day with strong winds is called a gale day. Gales can damage ground facilities and buildings, affecting operations such as navigation, offshore construction, and fishing; causing great harm; and making it a catastrophic weather event [5–8]. On 28 February 2007, a gale in Turpan caused a severe disaster of train rollover [9].

Turpan Basin, located in the east of Xinjiang, is the lowest depression in China. The Turpan Basin is a typical continental desert climate with closed terrain, drought and heat, scarce precipitation, windy and sandy weather, high evaporation, and extremely dry air. The special geographical conditions have created the special climatic characteristics of the Turpan Basin. It is famous for its high temperature, known as the "stove", with a maximum temperature of 48.0 °C [10].

Due to the influence of high temperature and dryness, Turpan has high fire potential. The occurrence of gales can not only transport oxygen to the ignition point to support combustion, but also blow burned objects onto other combustible materials, causing the fire to quickly spread and expand [11]. On 2 June 2004, the instantaneous maximum wind speed in the Turpan Basin reached 25 m/s from afternoon to evening. Due to the strong intensity, wide range, and sudden nature of this strong wind, roads were forced close and 32 fires were triggered, resulting in a direct economic loss of over CNY 30 million. On

22–23 April 2012, a gale in Turpan triggered 17 fire accidents, resulting in one death. Given the adverse effects of gales in Turpan, a hot and arid region, many studies have attempted to summarize the patterns of gales in this area. Ding et al. analyzed the dynamic mechanism of a typical mountain wind [12]. Chen et al. constructed a risk assessment model for gale disasters [13]. Li et al. explored the patterns and forecasting methods of strong winds in Turpan [14]. Generally speaking, the magnitude of wind depends on the pressure gradient force, which is determined by the atmospheric circulation. In addition, wind speed is closely related to terrain, especially in Turpan, a basin surrounded by mountains.

However, previous studies only analyzed the statistical laws of gales or provided the dynamic mechanism of only one strong wind process, without providing the basic characteristics of synoptic patterns during strong winds. Synoptic classification has been usually adapted to explore the possible meteorological causes related to a weather phenomenon [15]. Synoptic classification can be conducted through subjective and objective methods, with subjective methods based on prior standards, leading to large uncertainties. Compared to subjective circulation classification methods, objective classification methods can overcome the limitations of human experience and subjective judgment to process a large amount of data appropriately [16]. There are many objective classification methods, such as the correlation method [17], cluster analysis method [18,19], neural network method [20], nonlinear method [21,22], fuzzy classification method [23], and the t-mode principal component analysis using oblique rotation (T-PCA) method. Huth et al. compared these objective classification methods and found that the T-PCA method is the most efficient and accurate method to classify synoptic patterns in a defined region [15].

In this study, we examined the frequency and intensity changes of strong winds in the Turpan region from 2015 to 2021, and found that the directions of gales in the Turpan were all northwest and the occurrence of gales in winter was relatively rare. Furthermore, we explored the possible synoptic circulation types of gale events from the perspective of weather classification. The research results can provide references for the prevention of gale disasters in Turpan.

2. Materials and Methods

2.1. Study Area

This study covered the whole Turpan Basin, a typical graben basin, which is located at the southern slope of the eastern section of the Tianshan Mountains, with Bogda Mountain to the north and Kuruk Mountain to the south. The average altitude in the basin is about 400 m above sea level, while the altitudes of the plateaus and mountains are above 4000 m and 2000 m, respectively, as shown in Figure 1.

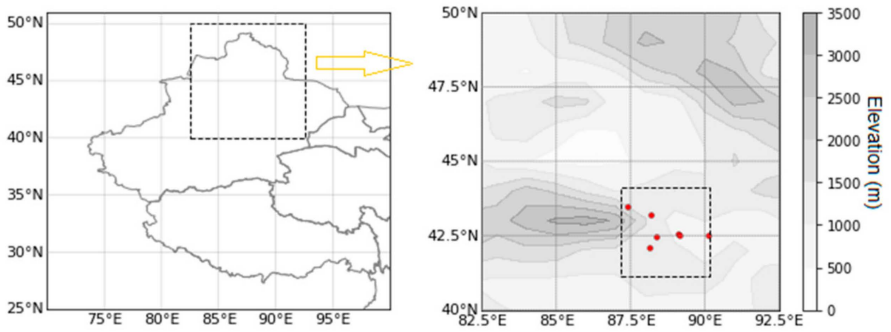

Figure 1. The location (**left panel**) and topography (**right panel**) of the Turpan Basin. In the left panel, the black square presents the region where the synoptic classification was conducted. In the right panel, the black square presents the location of Turpan Basin. The red dots present the location of seven stations.

2.2. Determination of Typical Strong Wind Processes

The hourly wind speed data of the seven sites in Turpan Basin from January 2015 to December 2019 were obtained from the China Meteorological Administration.

The frequency of strong winds does vary from station to station. To eliminate the impact of different strong wind frequencies between stations, the determination of typical strong wind processes is mainly divided into two steps [24].

The first step is to determine the month of the gale process. The frequency of different wind speeds ranging from 0 to 0.3, from 0.3 to 10.8, and above 10.8 m/s at each site are analyzed on the month scale. Furthermore, the months with maximum wind speeds greater than 10.8 m/s at most stations (the number of stations greater than or equal to 4) are selected as gale process months.

The second step is to reverse-check the historical hourly data based on the determined strong wind months, and select the processes with wind speeds above 10.8 m/s at most stations as the gale process. Figure 2 illustrates the detailed process for determining a gale process. To calculate the changes in physical quantities related to gales throughout the entire process, an additional 24 h will be added to the starting time and ending time of the entire process, respectively. There were 167 strong winds in Turpan from 2015 to 2021.

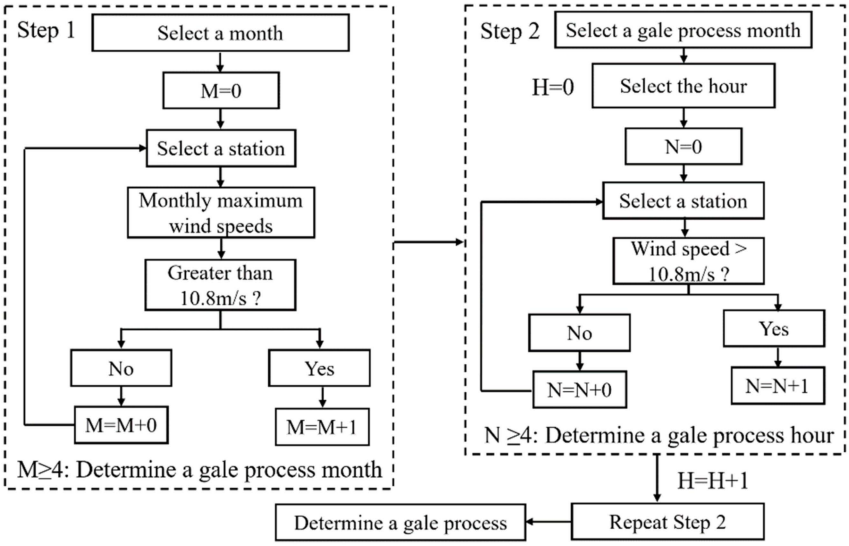

Figure 2. Flow chart of determining a gale process in Turpan Basin.

2.3. ERA5 Reanalysis Data

ERA5 dataset contains the fifth-generation atmospheric reanalysis data released by the European Center for Medium-Range Weather Forecasting (ECMWF). Compared with its previous generation, namely ERA-interim, the horizontal and vertical resolutions of ERA5 were significantly improved, and the performance of ERA5 was better in the evaluation of temperature, wind, humidity, and so on [25].

2.4. Objective Synoptic Classification

Due to the efficiency and accuracy, the T-PCA method was used to classify synoptic patterns in Turpan Basin in this paper. Similar to previous studies on circulation classification [26,27], the T-PCA method in this study is based on Cost733class software (http://cost733.met.no) (accessed on 20 October 2022), a piece of software developed by Earth System Science & Environmental Management and European Cooperation in Science & Technology, which includes the process of creating, comparing, and evaluating classification results [28,29]. This article mainly uses the T-PCA method to classify the synoptic patterns in the Turpan Basin and its surrounding areas (41.12–43.4° N, 87.16–91.55° E). The input data were the 850 hPa potential height field from ERA5 reanalysis data with a

spatial resolution of 0.25° × 0.25° at 14:00 BJT during 2015–2021. The cumulative explained variance was adopted for determining the number of principal components.

3. Results

3.1. Variations in the Occurrence of Gales

The variation in seasonal gales in the Turpan region is shown in Figure 3. Except for 2015 and 2017, the number of gales in spring, summer, and autumn was more than five times per year, while in winter, the gales occurred less than five times per year. The number of gales in winter was significantly lower, which was related to atmospheric circulation and is further analyzed next. From a seasonal perspective, spring and autumn showed an upward and then downward trend, with turning points in 2017 and 2018, respectively. Summer showed an upward trend, with a turning point in 2017. Although the frequency of gales in winter was relatively low, it has shown an upward trend since 2018.

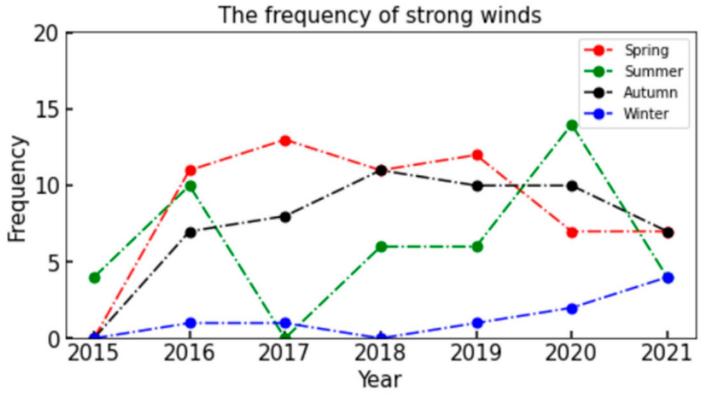

Figure 3. Annual changes in the frequency of strong winds in spring, summer, autumn, and winter in the Turpan region.

3.2. Synoptic Patterns

3.2.1. Identified Synoptic Patterns

By implementing the T-PCA classification method, the synoptic patterns in the Turpan Basin and the surrounding area were classified. Considering the impact of the number of principal components, we selected multiple principal components for sensitive analysis. The cumulative explained variance increases and then decreases with the number of principal components, reaching a maximum of nearly 80% when the number of classified types is nine, as shown in Figure 4. Therefore, the synoptic circulations in the Turpan Basin and its surrounding areas are classified into nine types in this paper, which is similar to previous studies [28,29].

The nine patterns were analyzed in this study, and their occurring days are shown in Table 1. The first synoptic pattern occurred in 417 days, out of 2557 days in total. The occurring days of types 2–9 were 479, 474, 263, 370, 221, 131, 152 and 50 days, respectively. Seasonally, type 3 almost evenly occurred throughout the four seasons. The occurrence frequencies of type 1 were highest in summer, but did not occur in winter. On the contrary, the occurrence frequencies of type 4 and type 8 were relatively higher in winter, followed by autumn, but close to zero in summer. Type 2 and type 5 occurred less frequently in winter than in the other three seasons. Type 6 almost occurred more frequently in winter, while type 7 almost occurred more frequently in spring. Therefore, we mainly discuss type 2, type 3, type 5 and type 7 in spring; type 1, type 2, type 3 and type 5 in summer; type 2–5 in autumn; as well as type 3, type 4, type 6 and type 8 in winter.

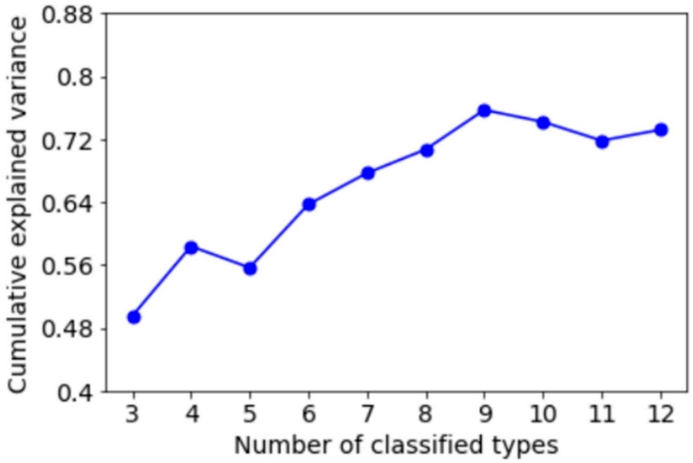

Figure 4. The number of classified types and corresponding cumulative explained variance.

Table 1. The occurring days of 6 synoptic patterns in four seasons from 2015 to 2021.

Type	Spring	Summer	Autumn	Winter
Type 1	51	317	49	0
Type 2	139	150	143	47
Type 3	130	46	187	111
Type 4	47	2	69	145
Type 5	156	78	76	60
Type 6	36	8	54	123
Type 7	60	35	23	13
Type 8	14	1	22	115
Type 9	11	7	14	18

The spatial distribution characteristics of 850 hPa potential heights for nine synoptic patterns are shown in Figure 5. In type 1, there was a higher-pressure center to the west and a lower-pressure center to the south, north as well as east of Turpan. Type 2 could be summarized as a higher-pressure center to the west and north, and a lower-pressure center to the south and east of Turpan. When type 3 occurred, there was a high-pressure center to the west of Turpan, and the pressure to the south of Turpan was relatively lower. In type 4, there was a strong high-pressure center to the east and south of the Turpan Basin. Moreover, the pressure to the north of Turpan was relatively lower. Type 5 was characterized by a lower-pressure center to the south and east of Turpan. In type 6, there was a strong high-pressure center to the south of the Turpan Basin. When type 7 occurred, there was a higher-pressure center to the west and north. In type 8, a strong high-pressure center was located at northeast of Turpan. Similar to type 3, type 9 could be summarized as a high-pressure center to the west of Turpan, and a relatively lower-pressure center to the south of Turpan. In general, in type 1, type 2, type 5 and type 7, there was a high-pressure center to the west and a lower-pressure center to the south of Turpan, although there are some differences in large-scale circulation systems under these classifications. When type 3 and type 9 occurred could be summarized as a high-pressure center to the west and a relatively lower-pressure center to the south of Turpan. Type 4, type 6 and type 8 were characterized by a strong high-pressure center to the south or northeast of the Turpan Basin.

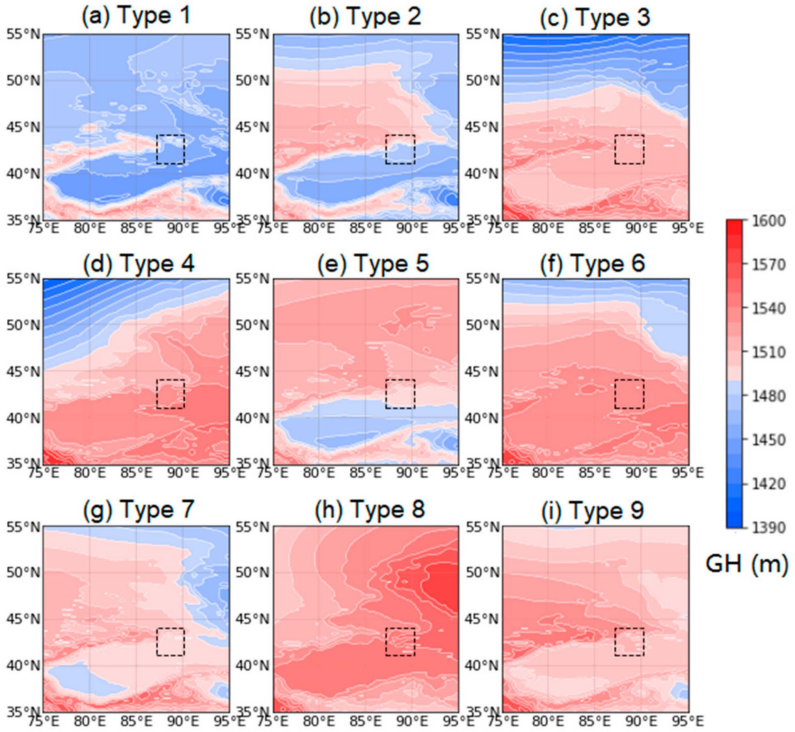

Figure 5. The distribution of geopotential heights at 850 hPa for the nine synoptic patterns in the Turpan Basin and its surrounding areas. The dashed boxes in the figure denote Turpan Basin.

3.2.2. The Impacts of Synoptic Patterns on Gales

The frequency and intensity of gales in Turpan for different synoptic patterns are shown in Figures 6 and 7, respectively.

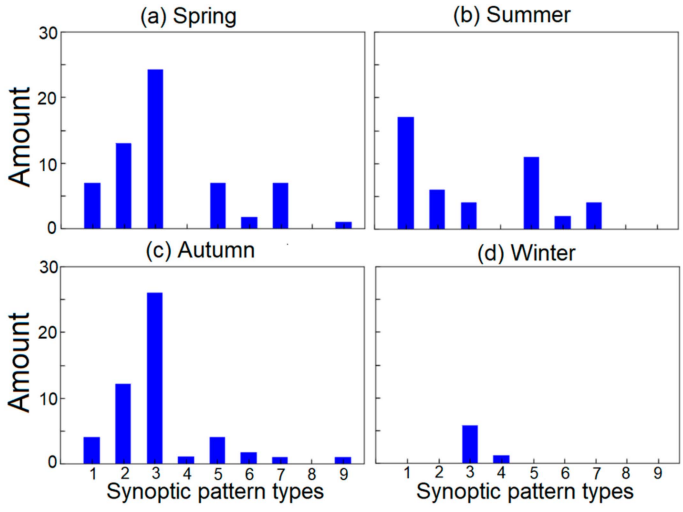

Figure 6. Frequency of gales for different synoptic patterns in the Turpan region.

In terms of the frequency of gales, in spring, no gales occurred in Turpan under type 4 and 8 patterns, while under type 6 and 9 patterns, gales occurred less frequently. However, gales occurred the most frequently under types 1, 2, 5, 7 and type 3, respectively. In summer, no gales occurred under type 4, 8 and 9 patterns, while under type 6, gales occurred less frequently. Gales occurred more frequently under type 2, 3, 5 and 1 patterns, respectively. In autumn, there was no strong wind in Turpan under type 8, while the frequency of gales was less frequent under type 1, 4, 6, 7 and 9 patterns. Gales occurred more and most

frequently under type 2 and 3 patterns, respectively. In winter, almost no gales occurred in the Turpan Basin, except under type 3.

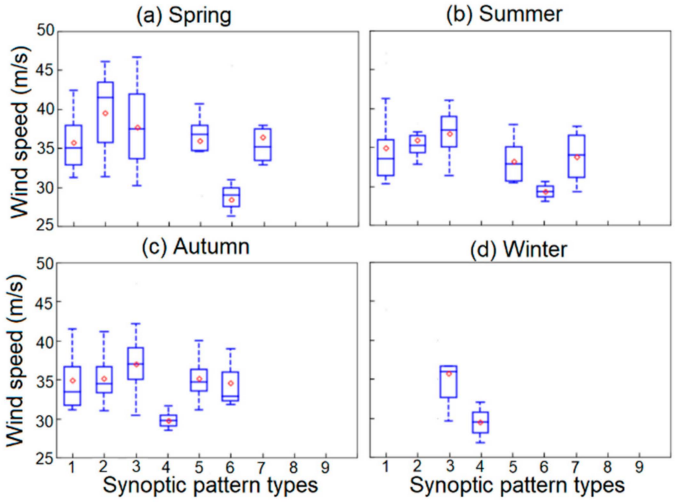

Figure 7. Intensity of gales for different synoptic patterns in the Turpan region.

In terms of intensity, under type 4 and 6 patterns, the amount of gales in Turpan was relatively small throughout the four seasons, with average wind speeds below 30 m/s. In spring, gales were the strongest under type 2, with average wind speeds of nearly 40 m/s. In summer, autumn and winter, gales were the strongest under type 3, with average wind speeds of above 35 m/s.

Considering the dominant patterns in the four seasons, gales mostly occurred under types 2 3, 5 and 7 in spring; types 1, 2, 3 and 5 in summer; types 2 and 3 in autumn, as well as type 3 in winter. It is noteworthy that all dominant synoptic patterns in spring and summer are prone to gales, indicating the importance of preventing gales during these seasons.

In addition to atmospheric circulation, terrain also plays an important role in affecting wind speeds. We extracted 10 m wind fields over the Turpan Basin in four seasons from ERA5 reanalysis data and superimposed the terrain. These wind fields for different dominant synoptic patterns (Figure 5) are shown in Figure 8a–d.

In spring (Figure 8a), under type 2, type 5 and type 7 patterns, there was a high-pressure center to the west and a lower-pressure center to the south of Turpan. Under type 3, the pressure to the west of Turpan was higher than that in Turpan, while the pressure to the south of Turpan was lower than that in Turpan (Figure 5). In these situations, the surface wind direction in Turpan was from northwest to southeast, due to the influence of pressure gradient force. Combined with the narrow pipe effect of the Tianshan Valley, it is easy to generate a northwest gale. Similarly, in summer (Figure 8b), under type 1, type 2, type 3 and type 5 patterns, the pressure to the west of Turpan had a high-pressure center, while the pressure to the south of Turpan was low (Figure 5). Therefore, the surface wind direction of the Turpan region is also northwest to southeast for all patterns.

In contrast, in autumn (Figure 8c) and winter (Figure 8d), for type 4, there was a strong high-pressure center to the southeast of Turpan, and the pressure to the north of Turpan was relatively lower (Figure 5d). The surface wind direction in Turpan was from south to north. For type 6, there was a strong high-pressure center to the south of the Turpan Basin, and the pressure to the northeast of Turpan was relatively lower (Figure 5f). The surface wind direction in Turpan was from southwest to northeast. For type 8 patterns, a strong high-pressure center was located over the northeast of Turpan, and the pressure to the southwest of Turpan was relatively lower (Figure 5h). The surface wind direction in Turpan was from northeast to southwest. However, due to the influence of the high terrain to the west of Turpan, the surface wind was blocked, and it seemed hard to form

gales. Figure 9 schematically shows the mechanism underlying the development of gales in response to various synoptic patterns combined with the terrain.

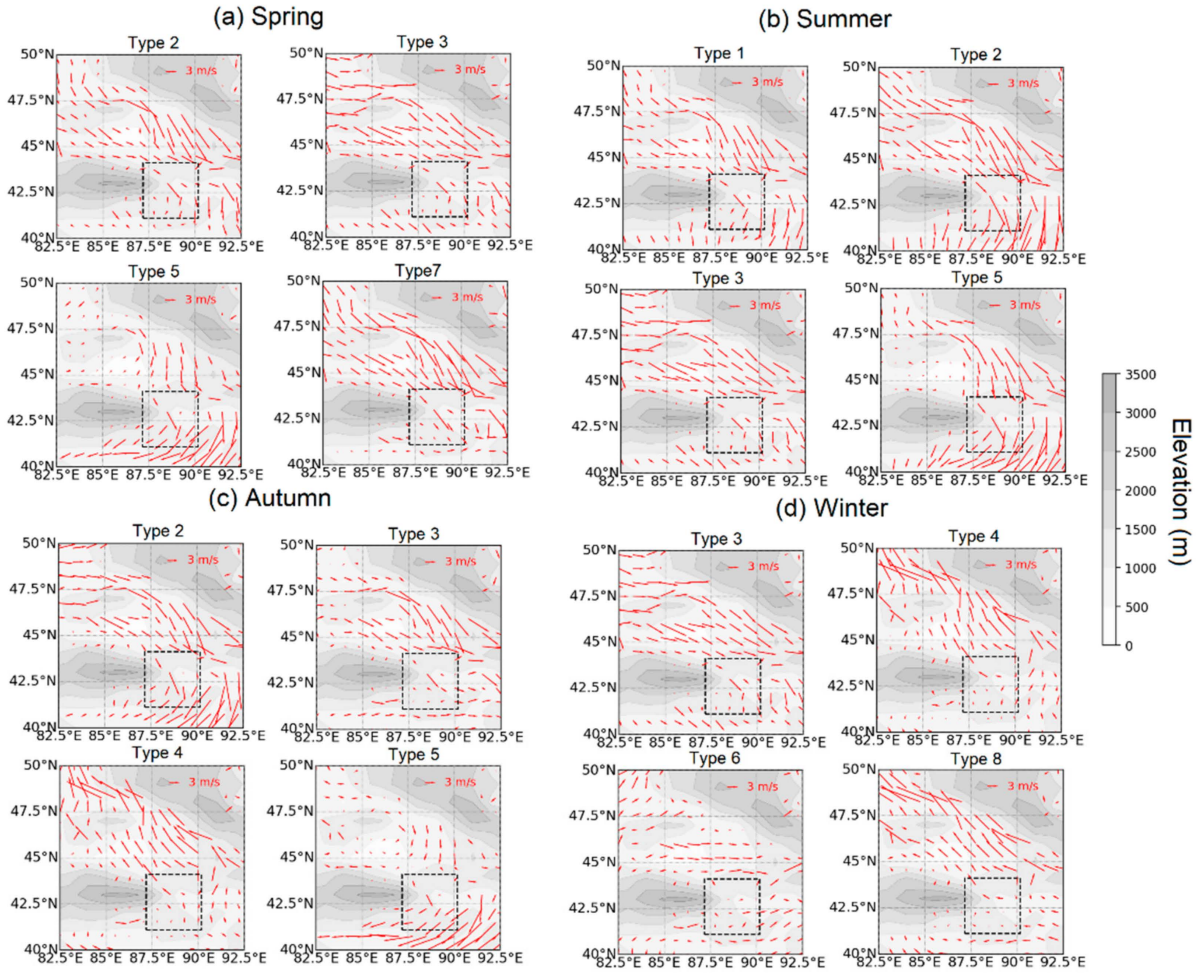

Figure 8. Ten-meter wind fields of different synoptic patterns for four seasons in Turpan and its surrounding areas. The dashed boxes in the figure denote Turpan Basin.

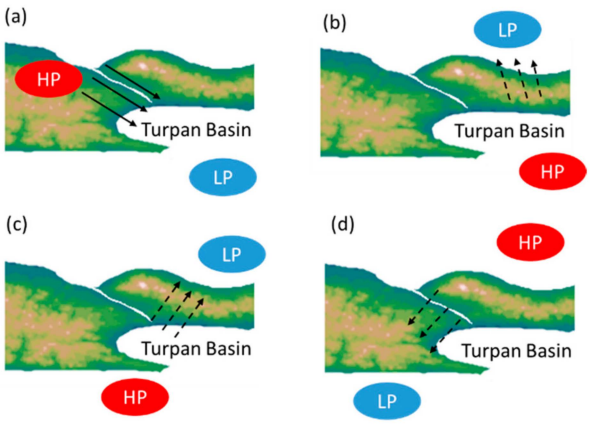

Figure 9. A schematic diagram describing the joint impacts of synoptic patterns and terrain on gales in Turpan Basin. The red and blue ovals represent higher and lower pressure centers, respectively. Solid and dashed lines represent wind strengthened and blocked by Tianshan Valley. (**a**) denotes types 1, 2, 3, 5 and 7. (**b**) denotes type 4. (**c**) denotes type 6. (**d**) denotes type 8.

4. Discussion

The synoptic patterns and their impacts on gales in the Turpan region were divided into nine synoptic patterns during 2015–2021 using the T-PCA method based on Cost733class software. It is worth noting that all the dominant patterns in spring and summer can incur gales, indicating the high frequencies of gales in spring and summer. However, the synoptic patterns in spring and summer need further analysis in the future to make gale prevention more effective.

Moreover, although the important impacts of large-scale synoptic forcing and topography on strong winds in Turpin have been emphasized in this study, the important roles of local atmospheric circulations cannot be overlooked. A mesoscale analysis of severe downslope windstorms revealed that when air parcels flow into the canyon due to the pressure gradient, lee waves and gap jets are formed by the asymmetric terrain and narrow pipe effect of Tianshan Valley, respectively. Lee waves transmit the energy of the gap jet to the ground, forming a downslope windstorm [9]. Moreover, local thermal instability will exacerbate the convective movement of the atmosphere over the basin, thereby rapidly enhancing the momentum spreading downward from higher levels and causing an increase in ground wind speed [30]. The impacts of local atmospheric circulations warrant further study and will form the basis of our future work.

In addition, in Turpan, a hot and arid region, with high fire potential, the occurrence of strong winds can exacerbate the impact of fires. Therefore, when higher pressure to the west and low pressure to the south of Turpan appears, special attention should be paid to fire protection. The extremely high-temperature disasters combined with gales should also be further explored.

5. Conclusions

Based on the observation data of seven stations in Turpan and ERA5 reanalysis data, this paper uses the T-PCA method to study the frequency and intensity of gales in Turpan from 2015 to 2021. Furthermore, the related synoptic patterns and mechanisms are explored. We find that the direction of gales in Turpan is basically from northwest to southeast, and the frequency of gales in winter is less than that in the other three seasons.

The synoptic patterns in the Turpan region can be roughly divided into nine synoptic patterns. Type 2, 3, 5 and 7; type 1, 2, 3 and 5; type 2, 3, 4 and 5; and type 3, 4, 6 and 8 synoptic patterns seem to be dominant in spring, summer, autumn and winter, respectively. For type 1, type 2, type 3, type 5, type 7 and type 9 patterns, there is a high-pressure center to the west and the pressure to the south of Turpan is relatively lower. In type 4, type 6 and type 8, there is a strong high-pressure center to the east of the Turpan Basin.

It is noteworthy that when the pressure to the west of Turpan is higher than that in Turpan, while the pressure to the south of Turpan is lower than that in Turpan, the surface wind direction in Turpan is from northwest to southeast. Combined with the narrow pipe effect of the Tianshan Valley, it is easy to generate a northwest gale. In contrast, if there is a strong high-pressure center to the south or northeast of Turpan, the surface wind is blocked due to the influence of the high terrain to the west and north of Turpan, and it seems hard to form a gale. Type 4, 6 and 8 patterns in winter account for over 60% of the total number of days, accounting for the fewest gales in Turpan during winter.

Author Contributions: Conceptualization, Z.X. and X.Z.; methodology, H.T.; software, H.H.; validation, Z.X. and X.Z.; resources, H.T.; data curation, H.T.; writing—original draft preparation, Z.X.; writing—review and editing, H.T.; visualization, H.T.; supervision, H.T.; project administration, H.H. and H.T.; funding acquisition, Z.X. and H.T. All authors have read and agreed to the published version of the manuscript.

Funding: This research was funded by the National Natural Science Foundation of China under grants 42165002, 42205040 and 42205170, and the Meteorological Development and Planning Institute Policy Research Program under grant ZCYJ2022006.

Institutional Review Board Statement: Not applicable.

Informed Consent Statement: Not applicable.

Data Availability Statement: Not applicable.

Conflicts of Interest: The authors declare no conflict of interest.

References

1. De, U.S.; Khole, M.; Dandekar, M.M. Natural hazards associated with meteorological extreme events. *Nat. Hazards* **2004**, *31*, 487–497. [CrossRef]
2. Zhou, L.; Wu, X.; Xu, Z.; Fujita, H. Emergency decision making for natural disasters: An overview. *Int. J. Disaster Risk Reduct.* **2018**, *27*, 567–576. [CrossRef]
3. de Freitas, A.A.; Oda, P.S.S.; Teixeira, D.L.S.; do Nascimento Silva, P.; Mattos, E.V.; Bastos, I.R.P.; Gonçalves, W.A. Meteorological conditions and social impacts associated with natural disaster landslides in the Baixada Santista region from March 2nd–3rd, 2020. *Urban Clim.* **2022**, *42*, 101110. [CrossRef]
4. Ma, X.; Liu, W.; Zhou, X.; Zhou, X.; Qin, C.; Chen, Y.; Xiang, Y.; Zhao, M. Evolution of online public opinion during meteorological disasters. *Environ. Hazards* **2020**, *19*, 375–397. [CrossRef]
5. Viúdez-Moreiras, D.; Gómez-Elvira, J.; Newman, C.E.; Navarro, S.; Marin, M.; Torres, J. Gale surface wind characterization based on the Mars Science Laboratory REMS dataset. Part I: Wind retrieval and Gale's wind speeds and directions. *Icarus* **2019**, *319*, 909–925. [CrossRef]
6. Huai, B.J.; Wang, Y.T.; Sun, W.J.; Wang, X.Y. The unique "Regional East Gale with Blowing Snow" natural disaster in Jeminay County, Xinjiang Uygur Autonomous Region, China. *Nat. Hazards* **2018**, *93*, 1105–1108.
7. Zhou, Q.J.; Li, L.; Chan, P.W.; Cheng, X.L.; Lan, C.X.; Su, J.C.; Yang, H.L. Observational Study of Wind Velocity and Structures during Supertyphoons and Convective Gales over Land Based on a 356-m-High Meteorological Gradient Tower. *J. Appl. Meteorol. Climatol.* **2023**, *62*, 103–118. [CrossRef]
8. Wang, Q.X.; Li, H.J. Analysis on gale disasters of Xinjiang in recent 40 years. *J. Desert Res.* **2003**, *23*, 545. (In Chinese)
9. Tang, H.; Lu, H.C.; Chu, C.J.; Sun, M.; Ju, C. Mesoscale analysis of severe downslope windstorm caused by gap jet in Tianshan Mountain canyon. *Meteorol. Mon.* **2020**, *46*, 1450–1460. (In Chinese)
10. Yang, L.; Fu, R.; He, W.; He, Q.; Liu, Y. Adaptive thermal comfort and climate responsive building design strategies in dry–hot and dry–cold areas: Case study in Turpan, China. *Energy Build.* **2020**, *209*, 109678. [CrossRef]
11. Falola, O.J.; Agbola, S.B. Institutional Capacity and the Roles of Key Actors in Fire Disaster Risk Reduction: The Case of Ibadan, Nigeria. *Int. J. Disaster Risk Sci.* **2022**, *13*, 716–728. [CrossRef]
12. Ding, J.; Chen, Y.; Wang, Y.; Xu, X. The southeasterly gale in Tianshan Grand Canyon in Xinjiang, China: A case study. *J. Meteorol. Soc. Jpn. Ser. II* **2019**, *97*, 55–67. [CrossRef]
13. Chen, B.; Wang, X.; Wang, X.; Zhou, S.; Gong, H. Assessment of Disaster Loss Index and Characteristics of Gale Disaster in Typical Arid and Semiarid Lands. *Discret. Dyn. Nat. Soc.* **2022**, *2022*, 9455559. [CrossRef]
14. Li, X.; Xia, X.; Zhong, S.; Luo, L.; Yu, X.; Jia, J.; Zhao, K.; Li, N.; Liu, Y.; Ren, Q. Shallow foehn on the northern leeside of Tianshan Mountains and its influence on atmospheric boundary layer over Urumqi, China—A climatological study. *Atmos. Res.* **2020**, *240*, 104940. [CrossRef]
15. Huth, R.; Beck, C.; Philipp, A.; Demuzere, M.; Ustrnul, Z.; Cahynová, M.; Tveito, O.E. Classifications of Atmospheric Circulation Patterns Recent Advances and Applications. *Trends Dir. Clim. Res.* **2008**, *1146*, 105–152.
16. Richman, M.B. Obliquely rotated principal components: An improved meteorological map typing technique? *J. Appl. Meteorol.* **1981**, *20*, 1145–1159. [CrossRef]
17. Lund, I.A. Map-Pattern classification by statistical methods. *J. Appl. Meteorol.* **1963**, *2*, 56–65. [CrossRef]
18. Brinkmann, W.A.R. Application of non-hierarchically clustered circulation components to surface weather conditions: Lake superior basin winter temperatures. *Theor. Appl. Climatol.* **1999**, *63*, 41–56. [CrossRef]
19. Cheng, F.F.; Zhao, J.S. Root cause diagnosis of disturbances propagation paths by using improved convergent cross mapping. *Comput. Aided Chem. Eng.* **2017**, *40*, 1693–1698.
20. Cassano, E.N.; Lynch, A.H.; Cassano, J.J.; Koslow, M.R. Classification of synoptic patterns in the western Arctic associated with extreme events at Barrow, Alaska, USA. *Clim. Res.* **2006**, *30*, 83–97. [CrossRef]
21. Hewitson, B.C.; Crane, R.G. Self-Organizing Maps: Applications to synoptic climatology. *Clim. Res.* **2002**, *22*, 13–26. [CrossRef]
22. Pezzi, L.P.; Cavalcanti, I.F.A. The relative importance of ENSO and tropical Atlantic sea surface temperature anomalies for seasonal precipitation over South America: A numerical study. *Clim. Dyn.* **2001**, *17*, 205–212. [CrossRef]
23. Bardossy, A.; Duckstein, L.; Bogardi, I. Fuzzy rule-based classification of atmospheric circulation patterns. *Int. J. Climatol.* **1995**, *15*, 1087–1097. [CrossRef]
24. Song, C.Y.; Yang, B.S. Gale disaster damage investigation process provement plan according to correlation analysis between wind speed and damage cost-Centering on disaster year book. *J. Korean Soc. Saf.* **2016**, *31*, 119–126. [CrossRef]
25. Hersbach, H.; Bell, B.; Berrisford, P.; Hirahara, S.; Horányi, A.; Muñoz-Sabater, J.; Thépaut, J.N. The ERA5 global reanalysis. *Q. J. R. Meteorol. Soc.* **2020**, *146*, 1999–2049. [CrossRef]
26. Miao, Y.; Guo, J.; Liu, S.; Liu, H.; Li, Z.; Zhang, W.; Zhai, P. Classification of summertime synoptic patterns in Beijing and their associations with boundary layer structure affecting aerosol pollution. *Atmos. Chem. Phys.* **2017**, *17*, 3097–3110. [CrossRef]

27. Ye, X.; Song, Y.; Cai, X.; Zhang, H. Study on the synoptic flow patterns and boundary layer process of the severe haze events over the North China Plain in January 2013. *Atmos. Environ.* **2016**, *124*, 129–145. [CrossRef]
28. Huth, R. A circulation classification scheme applicable in GCM studies. *Theor. Appl. Climatol.* **2000**, *67*, 1–18. [CrossRef]
29. Philipp, A.; Bartholy, J.; Beck, C.; Erpicum, M.; Esteban, P.; Fettweis, X.; Tymvios, F.S. Cost733cat—A database of weather and circulation type classifications. *Phys. Chem. Earth* **2010**, *35*, 360–373. [CrossRef]
30. Zhang, X.; Qu, X. Dynamical Mechanism of a Cross over Mountain Gale in Turpan. *Desert Oasis Meteorol.* **2006**, *29*, 21–23. (In Chinese)